Am J Transl Res 2019;11(12):7503-7522
www.ajtr.org /ISSN:1943-8141/AJTR0100171

Original Article

Identifying TF-miRNA-mRNA regulatory modules in nitidine chloride treated HCC xenograft of nude mice

Li Gao[1*], Dan-Dan Xiong[1*], Rong-Quan He[2], Ze-Feng Lai[5], Li-Min Liu[5], Zhi-Guang Huang[1], Xia Yang[1], Hua-Yu Wu[6], Li-Hua Yang[2], Jie Ma[2], Sheng-Hua Li[3], Peng Lin[4], Hong Yang[4], Dian-Zhong Luo[1], Gang Chen[1], Yi-Wu Dang[1]

Departments of [1]Pathology, [2]Medical Oncology, [3]Urology Surgery, [4]Ultrasound, First Affiliated Hospital of Guangxi Medical University, Nanning 530021, Guangxi Zhuang Autonomous Region, China; [5]School of Pharmacy, Guangxi Medical University, Nanning 530021, Guangxi Zhuang Autonomous Region, China; [6]Department of Cell Biology and Genetics, School of Pre-Clinical Medicine, Guangxi Medical University, Nanning 530021, Guangxi Zhuang Autonomous Region, China. [*]Equal contributors and co-first authors.

Received July 26, 2019; Accepted December 6, 2019; Epub December 15, 2019; Published December 30, 2019

Abstract: Nitidine chloride (NC) has reported tumor suppressive activities for various human cancers, including hepatocellular carcinoma (HCC). Nevertheless, the pharmacological mechanism of NC on HCC has not previously been elucidated. SMMC7721 HCC cell lines, before and after the treatment of NC, were injected into nude mice for a subcutaneous tumor xenograft model. MiRNA and mRNA sequencing were performed for both control and treated xenograft tissues to further analyze differential expressed miRNAs (DEmiRNAs) and mRNAs (DEmRNAs). The ten most significant DEmiRNAs were selected for prediction of transcription factors (TFs) and target genes. We constructed an interconnected network composed of TFs the ten most significant DEmiRNAs, the 100 most significant DEmRNAs, and selected target genes from online programs. Hub genes chosen from a protein-to-protein interaction network of hub genes were validated by correlation analysis, expression analysis, and Kaplan-Meier survival analysis. The five most up-regulated miRNAs (hsa-miR-628-5p, hsa-miR-767-5p, hsa-miR-767-3p, hsa-miR-1257, and hsa-miR-33b-3p) and the five most down-regulated miRNAs (hsa-miR-378d, hsa-miR-136-5p, hsa-miR-451a, hsa-miR-144-5p, and hsa-miR-378b) were singled out from the DEmiRNAs. Functional annotations indicated that potential target genes of the top five up-regulated miRNAs were mainly clustered in molecular processes concerning epithelial-to-mesenchymal transition. Hub genes, such as ITGA6 and ITGB4, were validated as up-regulated in HCC; both IFIT2 and IFIT3 were revealed by Kaplan-Meier survival curves as good prognostic factors for HCC. In summary, the regulating axes of NC-DEmiRNAs-DEmRNAs and TFs-DEmiRNAs-DEmRNAs in HCC that were discovered in this study may shed light on the possible molecular mechanism of NC in HCC.

Keywords: Nitidine chloride, hepatocellular carcinoma, xenograft, microRNA, transcription factor

Introduction

As one of the most common phenotypes of liver malignancies, hepatocellular carcinoma (HCC) takes a great toll on the health of people worldwide, especially in Asia and Africa [1]. Statistics of newly diagnosed cancer cases and new cancer deaths showed that HCC ranks as the sixth most common cancer diagnosis and the third most common cause of cancer-associated mortality [2]. Although therapeutic strategies, including resection, liver transplantation, image-guided tumor ablation, and transcatheter chemoembolization, have been developed to combat HCC, the clinical outcomes for HCC patients remain poor due to the lack of sensitive biomarkers for early detection and the obscure mechanisms underlying the carcinogenesis of HCC [3]. Therefore, it is imperative to uncover effective therapeutic targets for HCC and explore its complicated molecular basis.

Nitidine chloride (NC) is the primary active ingredient of the traditional Chinese medicine Zanthoxylum nitidum (Roxb) DC [4]. As a natural bioactive phytochemical alkaloid, NC is well known for diverse functions as an anti-fungal, anti-inflammatory, and anti-oxidant agent [5].

Recently, the tumor suppressive activities of NC have been proven for various human cancers, including HCC [6-8]. NC could inhibit tumor growth and stimulate apoptosis in HCC cells via disturbing relevant pathways [8, 9]. However, the pharmacological mechanism of NC in HCC has not yet been elucidated.

MicroRNAs (miRNAs), a class of short non-coding RNAs that post-transcriptionally regulate gene expression through inducing the degradation of target mRNAs or translational repression, are a hot research topic in cancer treatment because of their crucial roles as either oncogenes or tumor suppressors in a wide variety of cancers [10]. Dysregulation of multiple miRNAs in HCC, such as miR-34a,9 miR-506,10, miR-6451, miR-197,12 miR-552,13 and miR-65014, have been reported by previous studies [11]. However, the regulatory association between NC and miRNAs in HCC has not been researched. In the current study, we aimed to investigate potential NC-miRNA-mRNA axes in HCC by analyzing miRNA and mRNA expression profiles before and after NC treatment in HCC and to further investigate how these axes form interactive networks to impact the initiation and development of HCC.

Materials and methods

Human HCC nude mouse xenograft experiment

We have previously found the inhibitory effect of NC on growth of liver cancer cells [4, 12]. Male and female nude mice, purchased from Shanghai SLAC Laboratory Animal Co., Ltd. (Shanghai, China), were handled according to the Guide for the Care and Use of Laboratory Animals (the Shanghai SLAC Laboratory Animal of China, 2015). SMMC7721 cells (5×10^7 cells/L) were inoculated by subcutaneous injection into the right armpit of each mouse. When tumor size reached approximately 70 mm^3, all mice were randomly assigned to either the negative control group, which was intraperitoneally injected with saline, or the NC group, which was intraperitoneally injected with 7 mg/kg NC. After 15 days, the mice were anaesthetized, and the tumor tissues were excised and stored at -80°C.

RNA-seq

Total RNA was extracted with TRIzol Regent (Invitrogen, USA). RNA purity was detected using the NanoPhotometer® spectrophotometer (IMPLEN, CA, USA). RNA integrity was monitored using the RNA Nano 6000 Assay Kit of the Agilent Bioanalyzer 2100 system (Agilent Technologies, CA, USA).

The miRNA and mRNA sequencing libraries were established using the NEBNext® Multiplex Small RNA Library Prep Set for Illumina® (NEB, USA) and the rRNA-depleted RNA by NEB Next® Ultra™ Directional RNA Library Prep Kit for Illumina® (NEB, USA), respectively, following the manufacturer's recommendations. The library quality was monitored on the Agilent Bioanalyzer 2100 system. After removing reads with adaptors, >5% unknown nucleotides, and low-quality bases, qualified reads were mapped against human genome references (GRCh37/hg19).

Differential expression profiles

Prior to differential expression analysis, the raw count data of mRNA and miRNA sequencing in NC-treated and control samples was subjected to principal component analysis (PCA) in the lattice package of R software v.3.5.2 to examine outliers. After excluding samples containing outliers, we performed differential expression analysis utilizing the DESeq2 package in R software v.3.5.2 with raw count data of the remaining samples. The cutoff value for differentially expressed miRNAs (DEmiRNAs) and differentially expressed mRNAs (DEmRNAs) was set as log2-transformed fold change (FC) value >1 or <-1 and $P<0.05$.

TF predictions for the ten most significant DEmiRNAs

Transcription factors (TFs) are DNA-binding proteins that exert indispensable influence in regulating gene expression and cancer-associated pathways [13]. Mounting evidence suggests that some TFs interact with miRNAs to impact the transcriptome of target genes [14, 15]. In the present study, TFs that target the five most up-regulated miRNAs and five most down-regulated miRNAs, as ranked by *P*-value, were predicted by TransmiR v.2.0 and FunRich v.3.1.3. Both databases store regulatory relations between human TFs and miRNAs [16, 17]. Network diagrams and bar plots of predicted TFs were exported from TransmiR and FunRich, respectively.

Potential target genes of the ten most significant DEmiRNAs

One part of the target genes of the ten most significant DEmiRNAs was achieved from DEmRNAs in NC-treated human HCC xenografts in nude mice. Significantly up-regulated and down-regulated (|log2FC|>1, P<0.05) mRNAs corresponded to the target mRNAs of the five most down-regulated miRNAs and the five most up-regulated miRNAs, respectively. The target genes of the ten most significant miRNAs were also predicted by a combination of 12 online programs: miRWalk, Microt4, miRanda, mirbridge, miRDB, miRMap, miRNAMap, Pictar2, PITA, RNA22, RNAhybrid, and Targetscan. Genes frequently predicted by more than six online programs were selected as the target genes of the ten DEmiRNAs if they appeared as the common part of the prediction lists of the five most up-regulated or the five most down-regulated miRNAs. The potential target genes of the ten most significant DEmiRNAs came from the union of two parts. One part was the DEmRNAs in NC-treated human HCC xenografts in nude mice and the other part was predicted genes from online programs.

Functional analysis of the target genes of the ten most significant DEmiRNAs

After obtaining the target genes of the ten most significant DEmiRNAs, functional annotations composed of gene ontology (GO), Kyoto Encyclopedia of Genes and Genomes (KEGG) pathway, and disease ontology (DO) enrichment analyses were performed for these target genes to probe into their participation in biological processes and pathways. This was accomplished using the ClusterProfiler package of R software v.3.5.2. We constructed an interconnected network in Cytoskape v.3.7.0 to illustrate the interaction axes of TF-miRNA-mRNA. The interconnected network consisted of integrating predicted TFs simultaneously targeting more than four of the five most significantly up-regulated or down-regulated miRNAs, the ten most significant DEmiRNAs, the 100 most significant DEmRNAs, and selected target genes from online programs. Protein-to-protein interaction (PPI) networks were built for the target genes of the ten most significant DEmiRNAs to describe the interplay between target genes. From the PPI networks, hub genes that may play dominant roles were determined according to the connectivity degrees of the target genes.

Validations of hub genes

The level 3 IlluminaHiSeq expression profiles of hub genes in 423 The Cancer Genome Atlas (TCGA)-liver cancer and adjacent normal samples and level 3 IlluminaHiSeq expression profiles of the ten most significant DEmiRNAs in 420 TCGA-liver cancer and adjacent normal samples were downloaded from UCSC Xena (http://xena.ucsc.edu/) and paired to calculate the correlation between hub genes and the ten DEmiRNAs in HCC. Correlation analysis was conducted in GraphpadPrism v.8.0. Because of the imbalance in sample sizes between liver cancer and normal samples in TCGA, we additionally downloaded the transcripts per million (TPM) gene expression profiles of 175 normal liver samples from the Genotype-Tissue Expression (GTEx) database. The expression difference of eight TFs simultaneously targeting more than four of the five most significantly up-regulated or down-regulated miRNAs, hub genes in 373 HCC tissues, and 225 normal liver tissues from TCGA and GTEx were evaluated by students' t-tests and presented as scatterplots in GraphpadPrism v.8.0. From the eight TFs and ten hub genes, we chose ESR1 and ITGA6 for meta-analysis of differential expression based on microarray studies in Gene Expression Omnibus (GEO) database. We searched and included microarray studies with gene expression profiles of more than 20 HCC samples and more than 20 normal liver samples in the GEO database. The batch effect was removed for microarray studies from the same platform by the limma package in R software v.3.5.2. ITGA6 and ESR1 expression in HCC and normal samples was extracted from the included microarray datasets and log2 transformed when necessary. Forest plots of pooled standard mean difference (SMD) for ITGA6 and ESR1 expression in HCC and normal liver samples were created using meta and ggplot2 packages in R software v.3.5.2. We also referred to immunohistochemistry (IHC) data in the Human Protein Atlas (HPA) database to compare the protein expression of hub genes in HCC and normal hepatocytes. Kaplan-Meier Plotter (http://kmplot.com/analysis/) was utilized to assess the prognostic effect of hub genes on the over-

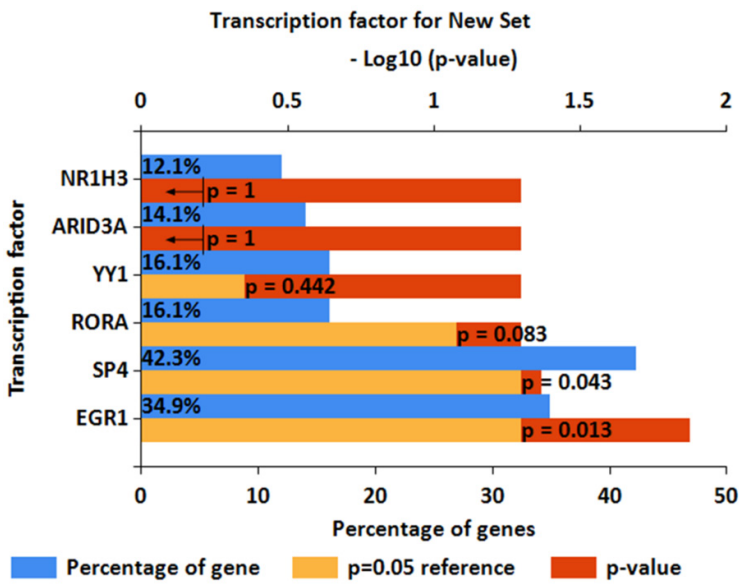

Figure 1. Transcription factors (TF) of the five most down-regulated miRNAs from FUNrich. Blue bars, orange bars, and red bars represent percentage of predicted genes, reference of P=0.05, and *p* value, respectively. SP4 and EGR1 were predicted to potentially target the five most down-regulated miRNAs (P=0.043; P=0.013).

all survival of 364 TCGA-LIHC patients and progress free survival of 370 TCGA-LIHC patients, split by the median expression value of hub genes. P<0.05 was considered statistically significant.

Results

DEmiRNAs in NC-treated samples

For in vitro experiment, NC successfully suppressed tumor growth in HCC nude mouse xenograft. Five samples including two control and three NC-treated samples were eligible for subsequent differential expression analysis after quality control of PCA. Differential expression analysis for the five samples revealed that a total of 10 miRNAs and 73 miRNAs were significantly up-regulated and down-regulated in NC-treated samples compared with control samples (|log2FC|>1, P<0.05) (Supplementary Figure 1). We focused on the five most up-regulated miRNAs (miR-628-5p, miR-767-5p, miR-767-3p, miR-1257, and miR-33b-3p) and the five most down-regulated miRNAs (miR-378d, miR-136-5p, miR-451a, miR-144-5p, and miR-378b) for further analysis. Differential expression of the five DEmiRNAs was exhibited in a panel of violin plots (Supplementary Figure 2).

Predicted TFs for the ten most significant DEmiRNAs

Prediction results from TransmiR for the ten most significant DEmiRNAs are shown in Supplementary Table 1. It can be observed that several TFs, such as CEBPB, MAX. KDM5B, and MAZ, could target up to four miRNAs (Supplementary Table 1). Two TFs (SP4 and EGR1) were predicted by FUNrich to potentially target the five most down-regulated miRNAs (P<0.05), while no results were returned for the five most up-regulated miRNAs (**Figure 1**).

DEmRNAs in NC-treated samples

Differential expression analysis for mRNA was performed on the three control tissues and two NC-treated tissues. Differential expression analysis for the five samples revealed that a total of 60 mRNAs and 137 mRNAs were significantly up-regulated and down-regulated in the NC-treated samples compared with the control samples (|log2FC|>1, P<0.05) (Supplementary Figure 3).

Potential target genes of the ten most significant miRNAs

The Venn plot in **Figure 2A** indicates that fifteen genes frequently predicted by six or more online programs, including PFKFB2, WWC2, PROX1, PTGER3, PURB, KLF12, ZAK, ALPK3, MKI67, IGF1R, ONECUT2, ARHGEF12, BBX, RAB3B, and CSNK1G1, were commonly part of the prediction lists of the five most significantly up-regulated miRNAs. As for the intersection results of the five most significantly down-regulated miRNAs, only one gene (LPP) was predicted by six or more online programs in the prediction lists of all the five most down-regulated miRNAs (**Figure 2B**). Taking DEmRNAs of NC-treated samples into account, a total of 152 genes and 61 genes were designated as the potential target genes of the five most significantly up-regulated and down-regulated genes, respectively.

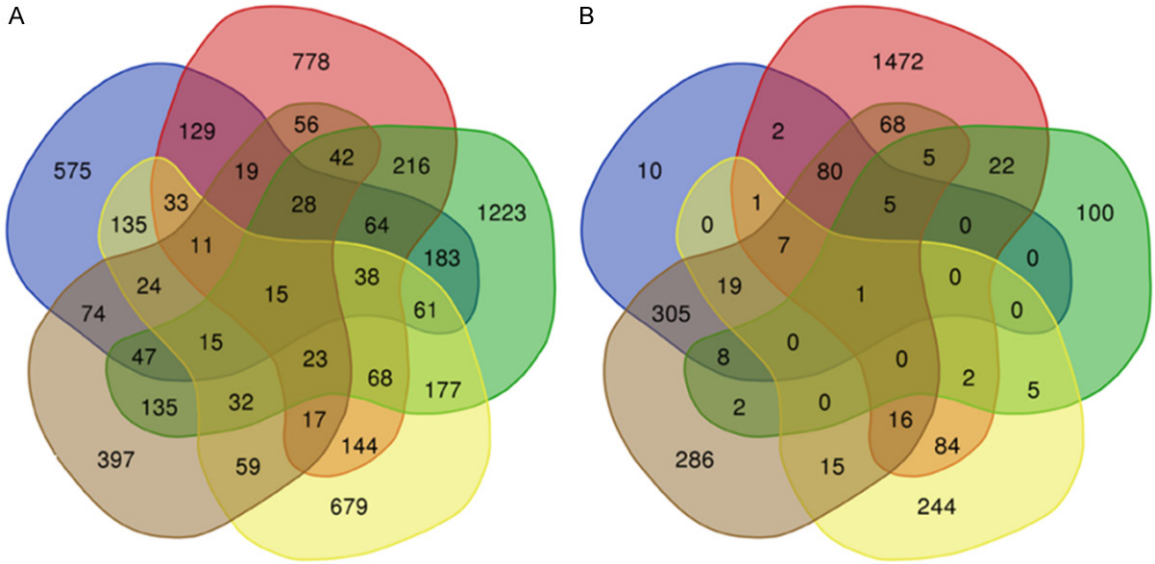

Figure 2. Venn plots of predicted target genes of the five top up-regulated miRNAs and the five top down-regulated miRNAs. A: Petals colored in blue, red, green, yellow, and brown mark predicted target genes of miR-628-5p, miR-767-5p, miR-767-3p, miR-1257, and miR-33b-3p. B: Petals colored in blue, red, green, yellow, and brown mark predicted target genes of miR-378d, miR-136-5p, miR-451a, miR-144-5p, and miR-378b.

Functional analysis of target genes of the ten most significant DEmiRNAs

GO and KEGG analyses for the target genes of the five most significantly up-regulated miRNAs suggested that these genes were remarkably assembled in biological processes, such as hemidesmosome assembly, cell junction organization, and renal system development ($P< 0.05$) (**Figure 3**; **Table 1**). Pathways that included arrhythmogenic right ventricular cardiomyopathy, cell adhesion molecules, and ECM-receptor interaction were significantly associated with these target genes ($P<0.05$) (**Figure 4**; **Table 1**). With respect to the target genes of the five most significantly down-regulated miRNAs, these genes prominently participated in biological processes in molecular functions, such as neurotransmitter receptor activity involved in regulation of postsynaptic membrane potential, transmitter-gated ion channel activity involved in regulation of postsynaptic membrane potential, and postsynaptic neurotransmitter receptor activity ($P<0.05$) (**Figure 5**; **Table 2**), as well as pathways including nicotine addiction, calcium signaling pathway, and EGFR tyrosine kinase inhibitor resistance (**Figure 6**; **Table 2**). DO analyses for target genes of the ten DEmiRNAs reached no significant terms.

The network diagrams consisting of predicted TFs simultaneously targeting more than four of the five most significantly up-regulated or down-regulated miRNAs, the ten most significant DEmiRNAs, the 100 most significant DEmRNAs, and selected target genes from online programs depicted the complicated interconnected relationships of the TF-miRNA-mRNA axis (**Figure 7**). According to the PPI networks for the target genes of the ten most significant DEmiRNAs, genes including ITGA6, LSR, KRT14, ITGB4, IFIT2, IFIT3, OASL, PDGFRB, CHRNA4, and LRRK2 with the highest connectivity degrees were selected as the hub genes (Supplementary Figure 4).

Validations of hub genes

Pearson correlation analyses based on expression data of hub genes and the ten most significant DEmiRNAs in HCC tissues reported a distinctly negative correlation between ITGA6, ITGB4, LRRK2, PDGFRB, miR-628-5p, miR-33b-3p, miR-1257, miR-378d, miR-451a, miR-144-5p, and miR-378b ($r<0$, $P<0.05$) (**Figure 8**). The RNA expression value of hub genes in HCC and normal samples from TCGA and GTEx reflected significant overexpression of ITGA6, LSR, KRT14, ITGB4, and LRRK2 in HCC tissues, which agreed with the anticipated oncogenic effect, because the five hub genes were five of

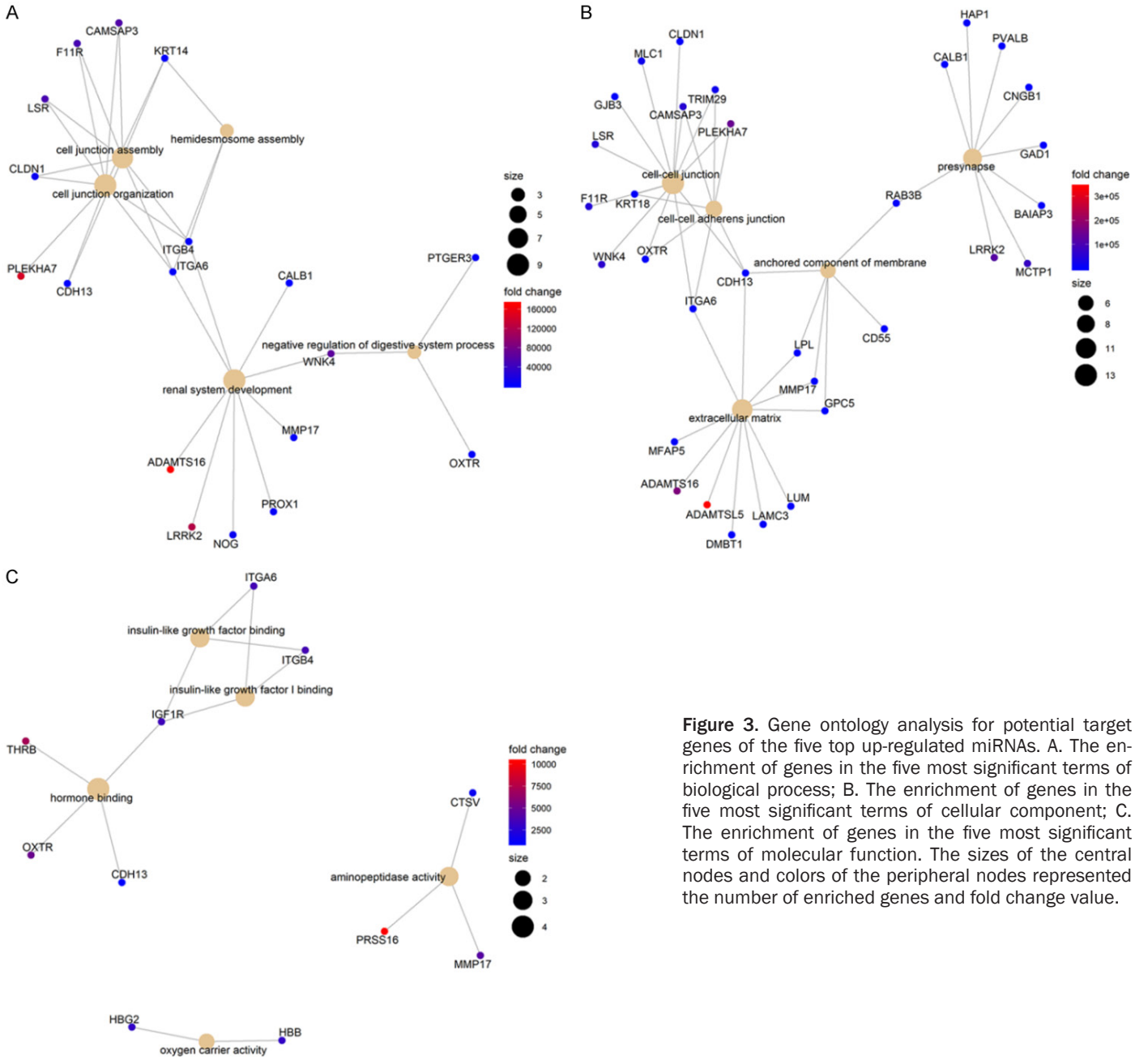

Figure 3. Gene ontology analysis for potential target genes of the five top up-regulated miRNAs. A. The enrichment of genes in the five most significant terms of biological process; B. The enrichment of genes in the five most significant terms of cellular component; C. The enrichment of genes in the five most significant terms of molecular function. The sizes of the central nodes and colors of the peripheral nodes represented the number of enriched genes and fold change value.

Table 1. GO and KEGG analysis for potential target genes of the five top up-regulated miRNAs

ID	Description	Gene Ratio	Bg Ratio	*P*-Value	P Adjust	Q Value	Gene ID	Count
GO:0031581	hemidesmosome assembly	3/128	11/17653	5.88848E-05	0.108413995	0.10328206	KRT14/ITGB4/ITGA6	3
GO:0034330	cell junction organization	9/128	270/17653	0.000156605	0.108413995	0.10328206	PLEKHA7/CAMSAP3/LSR/F11R/CLDN1/KRT14/ITGB4/ITGA6/CDH13	9
GO:0072001	renal system development	9/128	280/17653	0.000205479	0.108413995	0.10328206	ADAMTS16/LRRK2/WNK4/NOG/PROX1/MMP17/ITGB4/ITGA6/CALB1	9
GO:0034329	cell junction assembly	8/128	223/17653	0.000223071	0.108413995	0.10328206	CAMSAP3/LSR/F11R/CLDN1/KRT14/ITGB4/ITGA6/CDH13	8
GO:0060457	negative regulation of digestive system process	3/128	17/17653	0.000235069	0.108413995	0.10328206	WNK4/PTGER3/OXTR	3
GO:0005913	cell-cell adherens junction	7/134	110/18698	1.42939E-05	0.002074991	0.001781377	PLEKHA7/CAMSAP3/TRIM29/OXTR/KRT18/ITGA6/CDH13	7
GO:0005911	cell-cell junction	13/134	440/18698	1.70081E-05	0.002074991	0.001781377	PLEKHA7/WNK4/CAMSAP3/LSR/F11R/TRIM29/MLC1/CLDN1/OXTR/KRT18/ITGA6/GJB3/CDH13	13
GO:0031012	extracellular matrix	11/134	479/18698	0.000674451	0.051544312	0.044250725	ADAMTSL5/ADAMTS16/LAMC3/MFAP5/MMP17/LUM/LPL/ITGA6/GPC5/DMBT1/CDH13	11
GO:0031225	anchored component of membrane	6/134	159/18698	0.001008953	0.051544312	0.044250725	RAB3B/MMP17/LPL/GPC5/CD55/CDH13	6
GO:0098793	presynapse	9/134	379/18698	0.001657811	0.051544312	0.044250725	LRRK2/MCTP1/HAP1/BAIAP3/RAB3B/PVALB/GAD1/CNGB1/CALB1	9
GO:0031994	insulin-like growth factor I binding	3/129	13/17548	0.000105182	0.035446166	0.033325928	ITGB4/ITGA6/IGF1R	3
GO:0005520	insulin-like growth factor binding	3/129	29/17548	0.001233175	0.207789967	0.195360862	ITGB4/ITGA6/IGF1R	3
GO:0004177	aminopeptidase activity	3/129	45/17548	0.004396621	0.301461291	0.28342917	PRSS16/MMP17/CTSV	3
GO:0005344	oxygen carrier activity	2/129	14/17548	0.00460554	0.301461291	0.28342917	HBG2/HBB	2
GO:0042562	hormone binding	4/129	94/17548	0.005105336	0.301461291	0.28342917	THRB/OXTR/IGF1R/CDH13	4
hsa05412	Arrhythmogenic right ventricular cardiomyopathy (ARVC)	3/57	77/7867	0.018071713	0.624896034	0.620949322	ITGB4/ITGA6/CACNA2D1	3
hsa04514	Cell adhesion molecules (CAMs)	4/57	146/7867	0.021034104	0.624896034	0.620949322	F11R/CLDN1/ITGA6/ALCAM	4
hsa04512	ECM-receptor interaction	3/57	86/7867	0.02415834	0.624896034	0.620949322	LAMC3/ITGB4/ITGA6	3
hsa05410	Hypertrophic cardiomyopathy (HCM)	3/57	90/7867	0.027178083	0.624896034	0.620949322	ITGB4/ITGA6/CACNA2D1	3
hsa00250	Alanine, aspartate and glutamate metabolism	2/57	36/7867	0.027759351	0.624896034	0.620949322	RIMKLB/GAD1	2

Note: GO: Gene Ontology; KEGG: Kyoto Encyclopedia of Genes and Genomes. The top five significant terms (P<0.05) in each category were displayed.

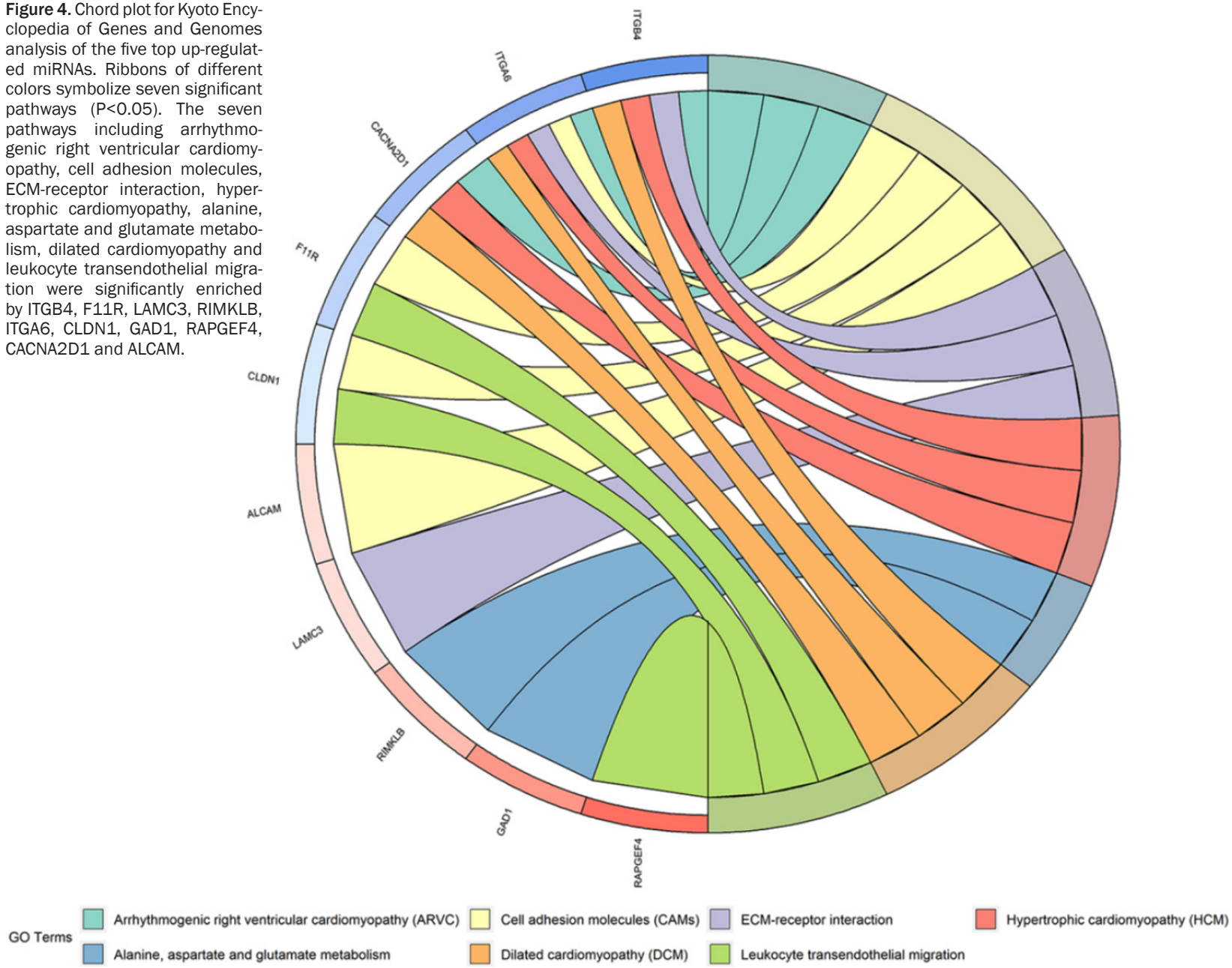

Figure 4. Chord plot for Kyoto Encyclopedia of Genes and Genomes analysis of the five top up-regulated miRNAs. Ribbons of different colors symbolize seven significant pathways ($P<0.05$). The seven pathways including arrhythmogenic right ventricular cardiomyopathy, cell adhesion molecules, ECM-receptor interaction, hypertrophic cardiomyopathy, alanine, aspartate and glutamate metabolism, dilated cardiomyopathy and leukocyte transendothelial migration were significantly enriched by ITGB4, F11R, LAMC3, RIMKLB, ITGA6, CLDN1, GAD1, RAPGEF4, CACNA2D1 and ALCAM.

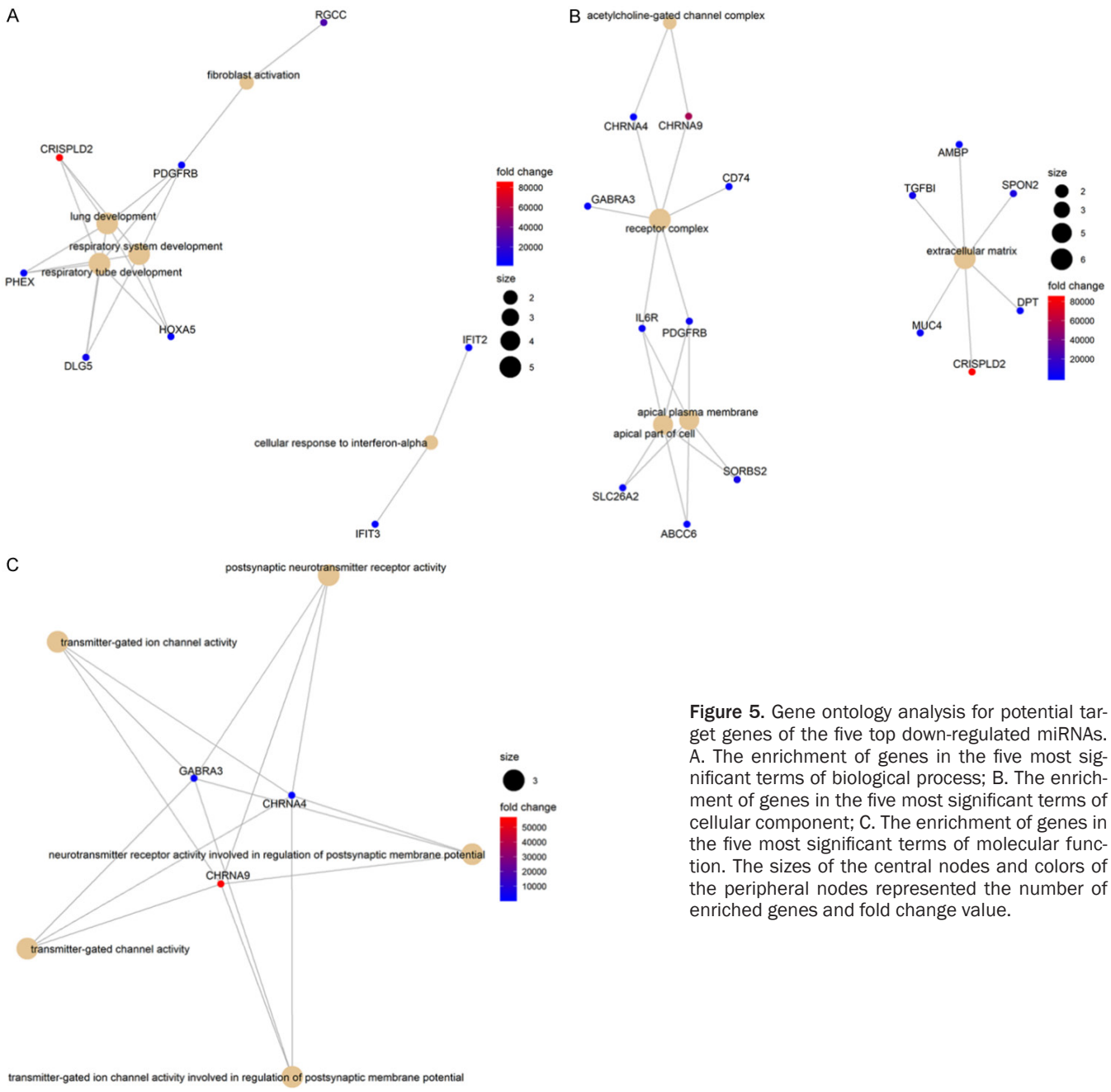

Figure 5. Gene ontology analysis for potential target genes of the five top down-regulated miRNAs. A. The enrichment of genes in the five most significant terms of biological process; B. The enrichment of genes in the five most significant terms of cellular component; C. The enrichment of genes in the five most significant terms of molecular function. The sizes of the central nodes and colors of the peripheral nodes represented the number of enriched genes and fold change value.

Table 2. GO and KEGG analysis for potential target genes of the five top down-regulated miRNAs

ID	Description	Gene Ratio	Bg Ratio	*P*-Value	P Adjust	Q Value	Gene ID	Count
GO:0030324	lung development	5/52	167/17653	0.000129477	0.086509579	0.076367812	CRISPLD2/DLG5/PHEX/PDGFRB/HOXA5	5
GO:0030323	respiratory tube development	5/52	171/17653	0.000144665	0.086509579	0.076367812	CRISPLD2/DLG5/PHEX/PDGFRB/HOXA5	5
GO:0060541	respiratory system development	5/52	193/17653	0.000254071	0.090234337	0.079655905	CRISPLD2/DLG5/PHEX/PDGFRB/HOXA5	5
GO:0035457	cellular response to interferon-alpha	2/52	10/17653	0.000377234	0.090234337	0.079655905	IFIT3/IFIT2	2
GO:0072537	fibroblast activation	2/52	10/17653	0.000377234	0.090234337	0.079655905	RGCC/PDGFRB	2
GO:0043235	receptor complex	6/54	374/18698	0.000706928	0.076385679	0.066604952	CHRNA9/PDGFRB/IL6R/GABRA3/CHRNA4/CD74	6
GO:0005892	acetylcholine-gated channel complex	2/54	18/18698	0.001215951	0.076385679	0.066604952	CHRNA9/CHRNA4	2
GO:0016324	apical plasma membrane	5/54	300/18698	0.001710127	0.076385679	0.066604952	SORBS2/PDGFRB/IL6R/SLC26A2/ABCC6	5
GO:0031012	extracellular matrix	6/54	479/18698	0.002498882	0.083712541	0.072993653	CRISPLD2/SPON2/TGFBI/MUC4/DPT/AMBP	6
GO:0045177	apical part of cell	5/54	366/18698	0.004029599	0.099719836	0.08695131	SORBS2/PDGFRB/IL6R/SLC26A2/ABCC6	5
GO:0099529	neurotransmitter receptor activity involved in regulation of postsynaptic membrane potential	3/51	38/17548	0.00018159	0.014755691	0.012039395	CHRNA9/GABRA3/CHRNA4	3
GO:1904315	transmitter-gated ion channel activity involved in regulation of postsynaptic membrane potential	3/51	38/17548	0.00018159	0.014755691	0.012039395	CHRNA9/GABRA3/CHRNA4	3
GO:0098960	postsynaptic neurotransmitter receptor activity	3/51	40/17548	0.000211804	0.014755691	0.012039395	CHRNA9/GABRA3/CHRNA4	3
GO:0022824	transmitter-gated ion channel activity	3/51	57/17548	0.000605831	0.025323722	0.020662015	CHRNA9/GABRA3/CHRNA4	3
GO:0022835	transmitter-gated channel activity	3/51	57/17548	0.000605831	0.025323722	0.020662015	CHRNA9/GABRA3/CHRNA4	3
hsa05033	Nicotine addiction	2/21	40/7867	0.004980053	0.33252323	0.314514725	GABRA3/CHRNA4	2
hsa04020	Calcium signaling pathway	3/21	193/7867	0.013962079	0.33252323	0.314514725	CACNA1I/PDGFRB/PDE1A	3
hsa01521	EGFR tyrosine kinase inhibitor resistance	2/21	79/7867	0.018480044	0.33252323	0.314514725	PDGFRB/IL6R	2
hsa04742	Taste transduction	2/21	83/7867	0.020281396	0.33252323	0.314514725	PDE1A/GABRA3	2
hsa05032	Morphine addiction	2/21	91/7867	0.024095886	0.33252323	0.314514725	PDE1A/GABRA3	2

Note: GO: Gene Ontology; KEGG: Kyoto Encyclopedia of Genes and Genomes. The top five significant terms ($P<0.05$) in each category were displayed.

Differential expressed miRNAs and mRNAs related to NC in HCC

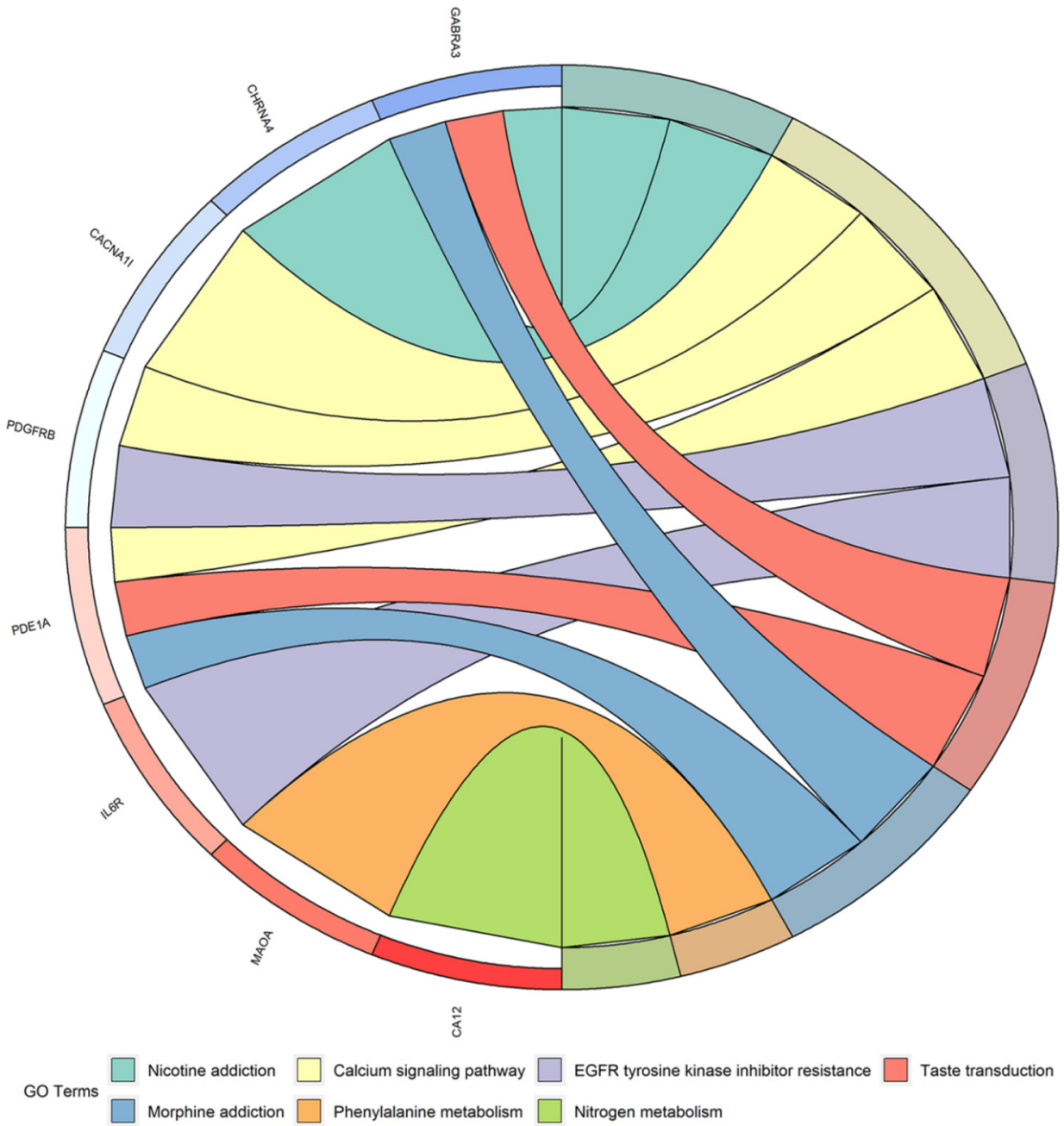

Figure 6. Chord plot for Kyoto Encyclopedia of Genes and Genomes analysis of the five top down-regulated miRNAs. Ribbons of different colors symbolize seven significant pathways (P<0.05). The seven pathways including nicotine addiction, calcium signaling pathway, EGFR tyrosine kinase inhibitor resistance, taste transduction, morphine addiction, phenylalanine metabolism and nitrogen metabolism were significantly enriched by GABRA3, CACNA1I, PDGFRB, PDE1A, MAOA, CA12, CHRNA4 and IL6R.

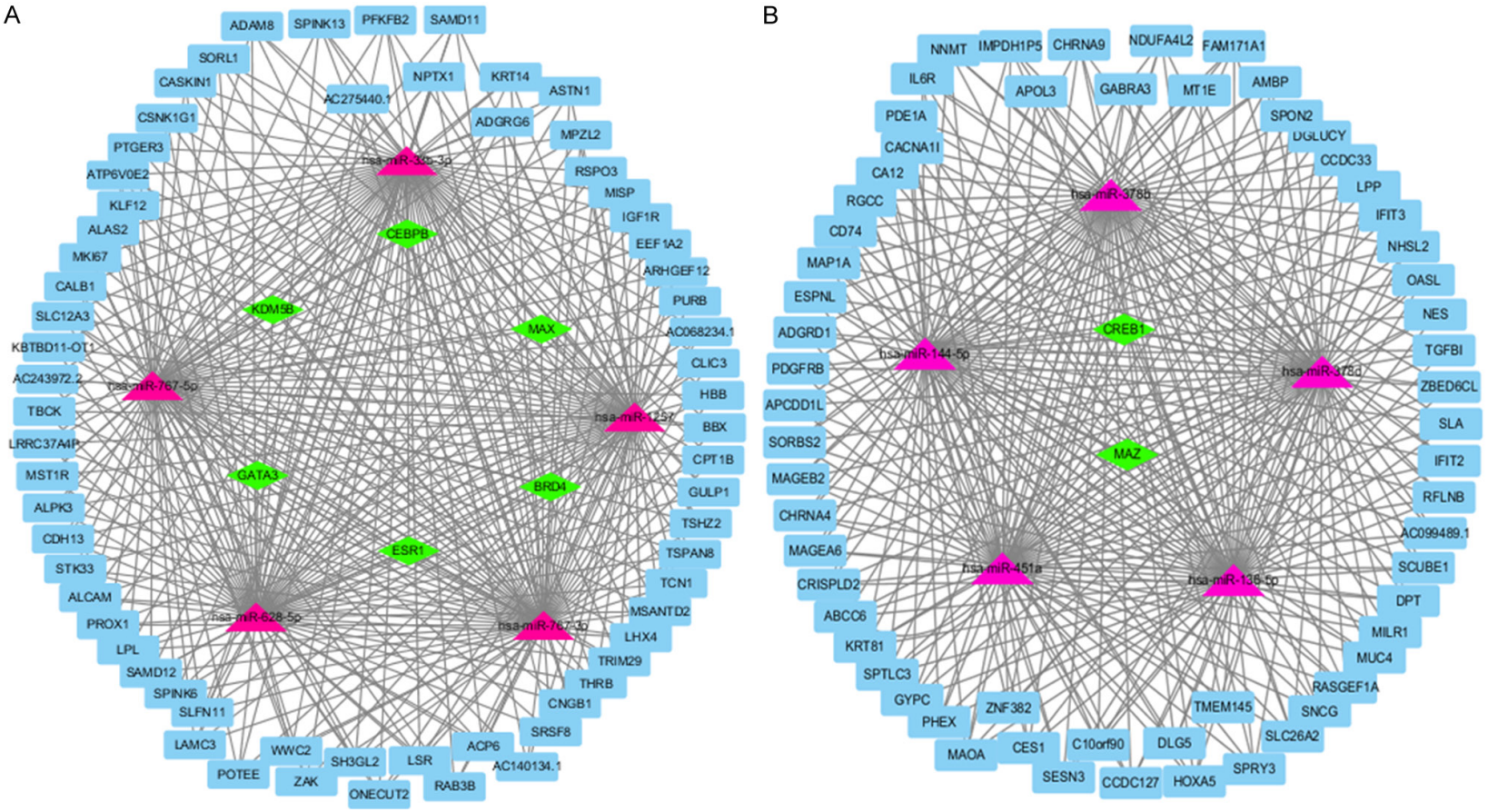

Figure 7. Interconnected networks of transcription factors (TF), differentially expressed miRNAs (DEmiRNA), and differentially expressed mRNAs (DEmRNAs). A: Predicted TFs simultaneously targeting more than four of the five most significantly up-regulated miRNAs, the five most significant up-regulated DEmiRNAs, the 50 most significant down-regulated DEmRNAs, and selected target genes from online programs are marked in green, red, and blue, respectively. B: Predicted TFs simultaneously targeting more than four of five most significantly down-regulated miRNAs, the five most significant down-regulated DEmiRNAs, the 50 most significant up-regulated DEmRNAs, and selected target genes from online programs are marked in green, red, and blue, respectively.

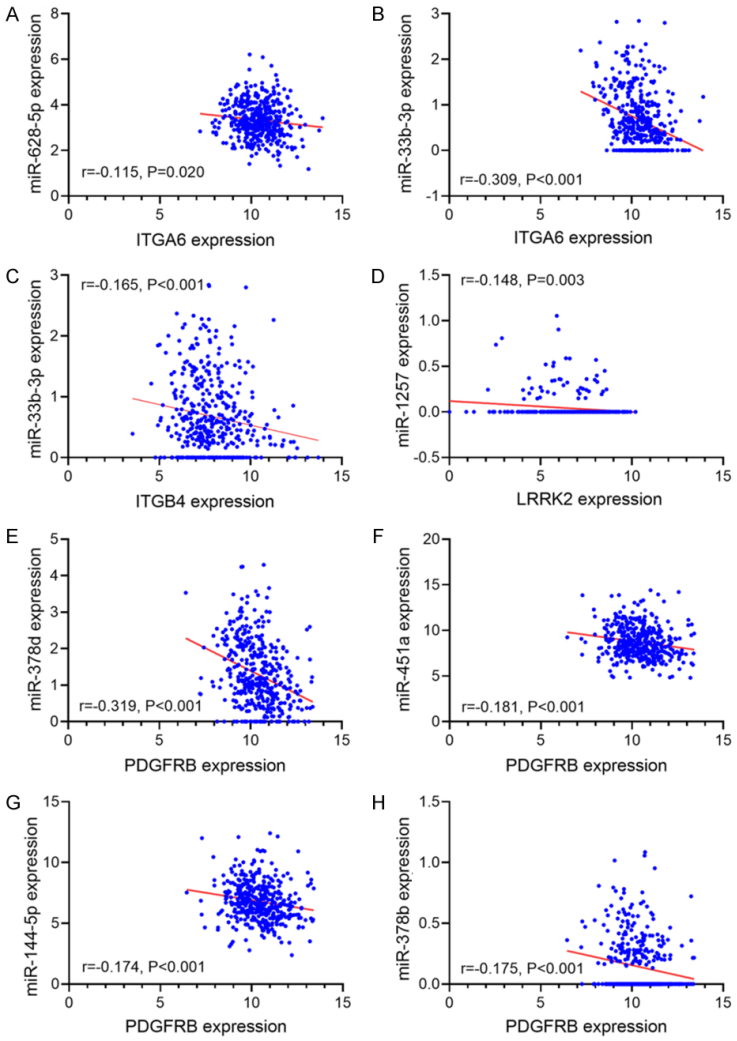

Figure 8. Correlation diagrams of hub genes and DEmiRNAs. (A) miR-628-5p-ITGA6 correlation pair; (B) miR-33b-3p-ITGA6 correlation pair; (C) miR-33b-3p-ITGB4 correlation pair; (D) miR-1257-LRRK2 correlation pair; (E) miR-378d-PDGFRB correlation pair; (F) miR-451a-PDGFRB correlation pair; (G) miR-144-5p-PDGFRB correlation pair; and (H) miR-378b-PDGFRB correlation pair.

the down-regulated DEmRNAs after the treatment of NC in xenograft tumors of nude mice (Supplementary Figure 5I-L and 5R).

A total of 20 GEO microarray studies containing 1836 HCC samples and 1554 normal samples were included for meta-analysis. Trends of increased expression of ITGA6 and decreased expression of ESR1 (**Figure 9**) could be observed in the forest plots, corresponding to the anticipated oncogenic effect of ITGA6. IHC images in the HPA database evidenced higher expression of ITGA6, LSR, and LRRK2 in HCC cells than in normal hepatocytes and lower expression of IFIT3 in HCC cells than in normal hepatocytes (**Figure 10**). Kaplan-Meier survival curves indicated an improved survival outcome for HCC patients with lower expression of ITGA6 and higher expression of IFIT2, IFIT3, OASL, PDGFRB and CHRNA4 ($P<0.05$), supporting the carcinogenic effect of ITGA6 and anti-tumor effect of IFIT2, IFIT3, OASL, PDGFRB and CHRNA4 for HCC (**Figures 11** and **12**).

Discussion

The regulatory relationship between NC and miRNA has rarely been reported. Through literature investigation, we only found one study by Liu N et al. that pertained to how NC mediated c-Myc-activated miRNAs in chronic myeloid leukemia (CML) [18]. The current work pioneers investigation of the miRNA and mRNA expression profiles of human HCC xenografts in nude mice treated with NC.

As shown by the differential expression profiles, multiple miRNAs were involved with NC in HCC. To facilitate the research, emphasis was placed on the top five up-regulated and down-regulated miRNAs. Among the five top up-regulated miRNAs, miR-767-3p was reported to be inhibited by hsa_circ_0000673 in the malignant progression of HCC [19], which evidenced the expected tumor-suppressive effect of miR-767-3p. The other four top up-regulated miRNAs have not been studied in HCC by previous researchers. Regarding the top five down-regulated miRNAs, two of them (miR-136-5p and hsa-miR-451a) have documented research. However, both studies related to miR-136-5p and miR-451a in HCC pointed out the carcinostatic functions of miR-136-5p and miR-451a in HCC [20, 21], contradictory with the expected oncogenic functions of them. This might be attributed to the following causes. Firstly, the human HCC xenograft in nude mice

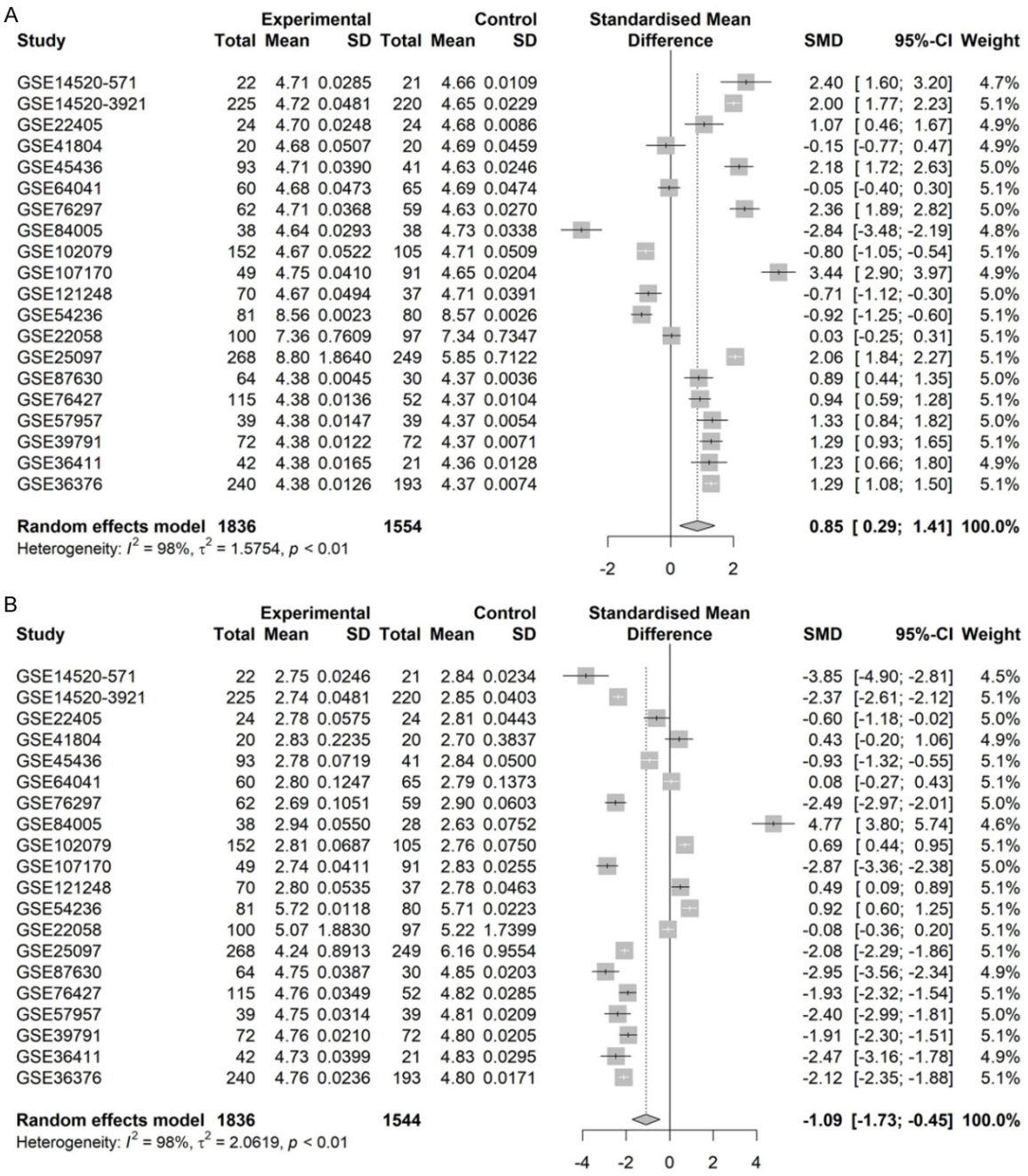

Figure 9. Forest plot of ITGA6 and ESR1 expression in hepatocellular carcinoma (HCC) and normal tissues from microarray studies. A. Pooled standard mean difference (SMD) of ITGA6 expression between HCC and normal tissues. B. Pooled SMD of ESR1 expression between HCC and normal tissues.

originated from a single cell line, SMMC7721. A single cell line could not wholly represent the biological background of HCC tissues in human. Secondly, the molecular mechanism of miR-136-5p and miR-451a in HCC by the two studies was unable to reflect the molecular basis of miR-136-5p and miR-451a regulated by NC in SMMC7721 cell lines.

A comprehensive study of the molecular mechanism of miRNAs in cancer should embrace both the upstream and downstream transcription. TFs have crucial actions on the transcription regulation of genes via binding to the promoters and distal cis-regulatory elements [13]. The onset of carcinogenesis in a wide type of human cancers could be related to abnormal

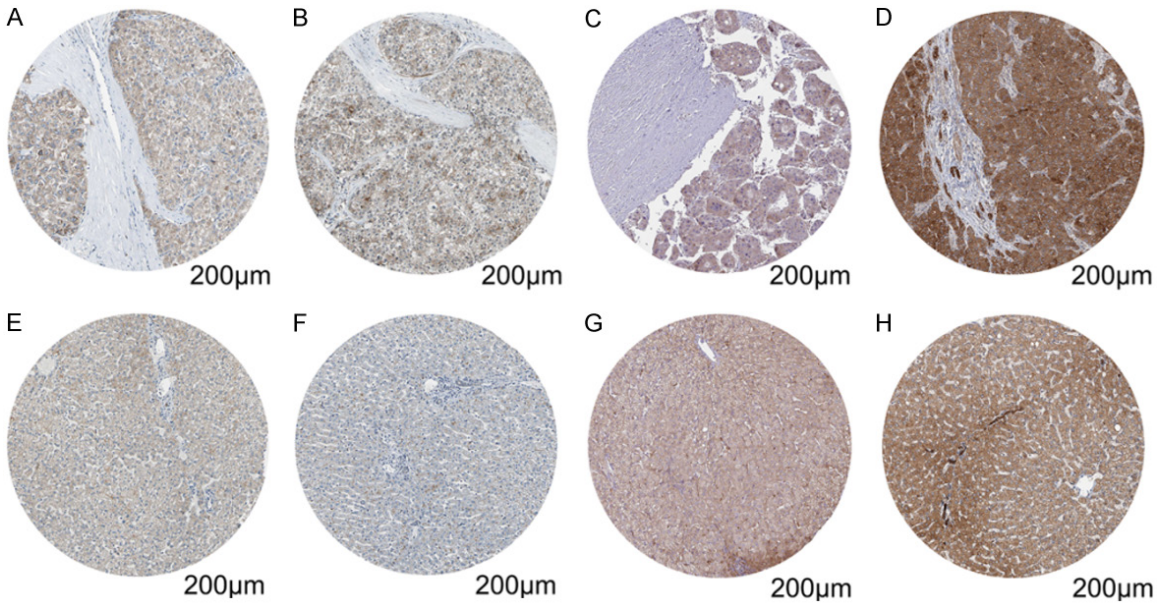

Figure 10. Immunohistochemistry images of ITGA6, LSR, IFIT3, and LRRK2 in hepatocellular carcinoma (HCC) and normal tissues from HPA database. A: Intermediate immunostaining of ITGA6 in HCC cells (antibody CAB009009); B: Immunostaining of ITGA6 in normal hepatocytes was not detected (antibody CAB009009); C: Intermediate immunostaining of LSR in HCC cells (antibody HPA007270); D: Low immunostaining of LSR in normal hepatocytes (antibody HPA007270); E: Low immunostaining of IFIT3 in HCC cells (antibody HPA059914); F: Intermediate immunostaining of IFIT3 in normal hepatocytes (antibody HPA059914); G: High immunostaining of LRRK2 in HCC cells (antibody CAB037160); H: Intermediate immunostaining of LRRK2 in normal hepatocytes (antibody CAB037160).

TF-driven proceedings [22-24]. Thus, it is worthwhile to predict TFs that target the ten most significant DEmiRNAs. A great number of TFs were reaped from the prediction of TransmiR and FUNrich. Particularly, several TFs with reported tumor-promoting or tumor-suppressing effects in HCC, such as MAZ, CREB1, ESR1, CEBPB, and KDM5B, were predicted to target four of the five top down-regulated or up-regulated miRNAs [25-29]. We hypothesized that these TFs might be engaged in NC-induced expression change of the ten most significant miRNAs at the transcription level. Specifically, one of the TFs, ESR1, was validated by meta-analysis of microarray studies to be down-regulated in HCC samples, consistent with reported research [30]. ESR1 was predicted by TransmiR to target four of the five top up-regulated miRNAs, which hinted at the positive regulatory relationship between ESR1 and the five top up-regulated miRNAs.

After prediction of TFs, we devoted attention to the downstream target genes of the ten most significant DEmiRNAs. It was noted that GO and KEGG terms containing key words such as “cell junction” and “cell adhesion” were frequently clustered by potential target genes of the top five up-regulated miRNAs, which implied that these target genes were active in epithelial-to-mesenchymal transition (EMT)-related programs. In the study of Sun M et al., NC was demonstrated to impair the EMT- and cancer stem cell-like properties of breast cancer cells through interfering with Hedgehog pathway [31]. NC also possesses inhibitory effects on the EMT of osteosarcoma cells through acting on Akt/GSK-3β/Snail signaling pathway [32]. We assumed that NC might trigger overexpression of the top five up-regulated miRNAs to restrain the EMT activities participated by target genes, thus opposing the initiation and development of HCC. We further narrowed down the research focus to concentrate on hub genes, because these genes, with highest connecting degrees in PPI networks, may have key functions. In line with our assumptions, two of the hub genes of the top five up-regulated miRNAs were declared to promote the progression of HCC, while two of the hub genes of the top five down-regulated miRNAs were found to be protective factors in HCC prevention. The in vitro experiments led by Lv. et al. showed that short hairpin RNA silence-targeting ITGA6 could

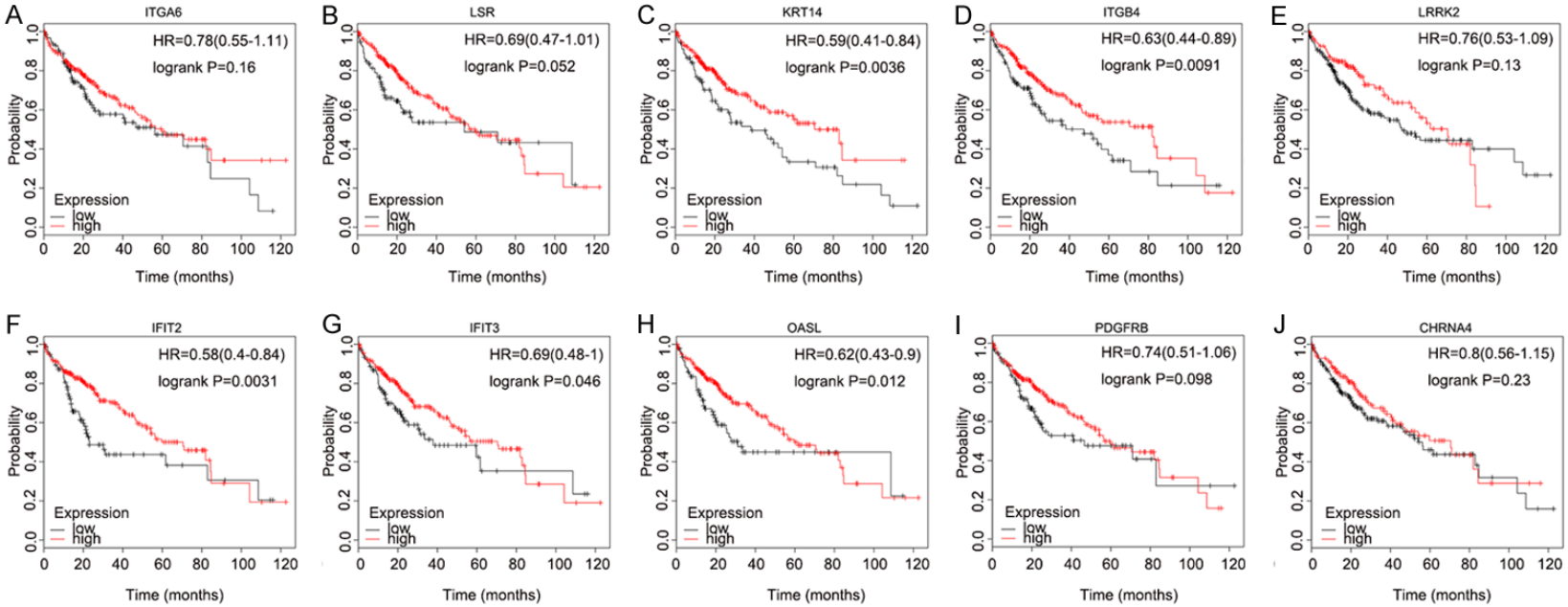

Figure 11. Kaplan-Meier survival curves for the prognostic significance of ten hub genes on overall survival of liver cancer patients from the Cancer Genome Atlas. Liver cancer patients were split by the median expression value of hub genes. HR: hazard ratio. The survival outcome of patients in high expression group was marked in red line while the survival outcome of patients in low expression group was marked in black line.

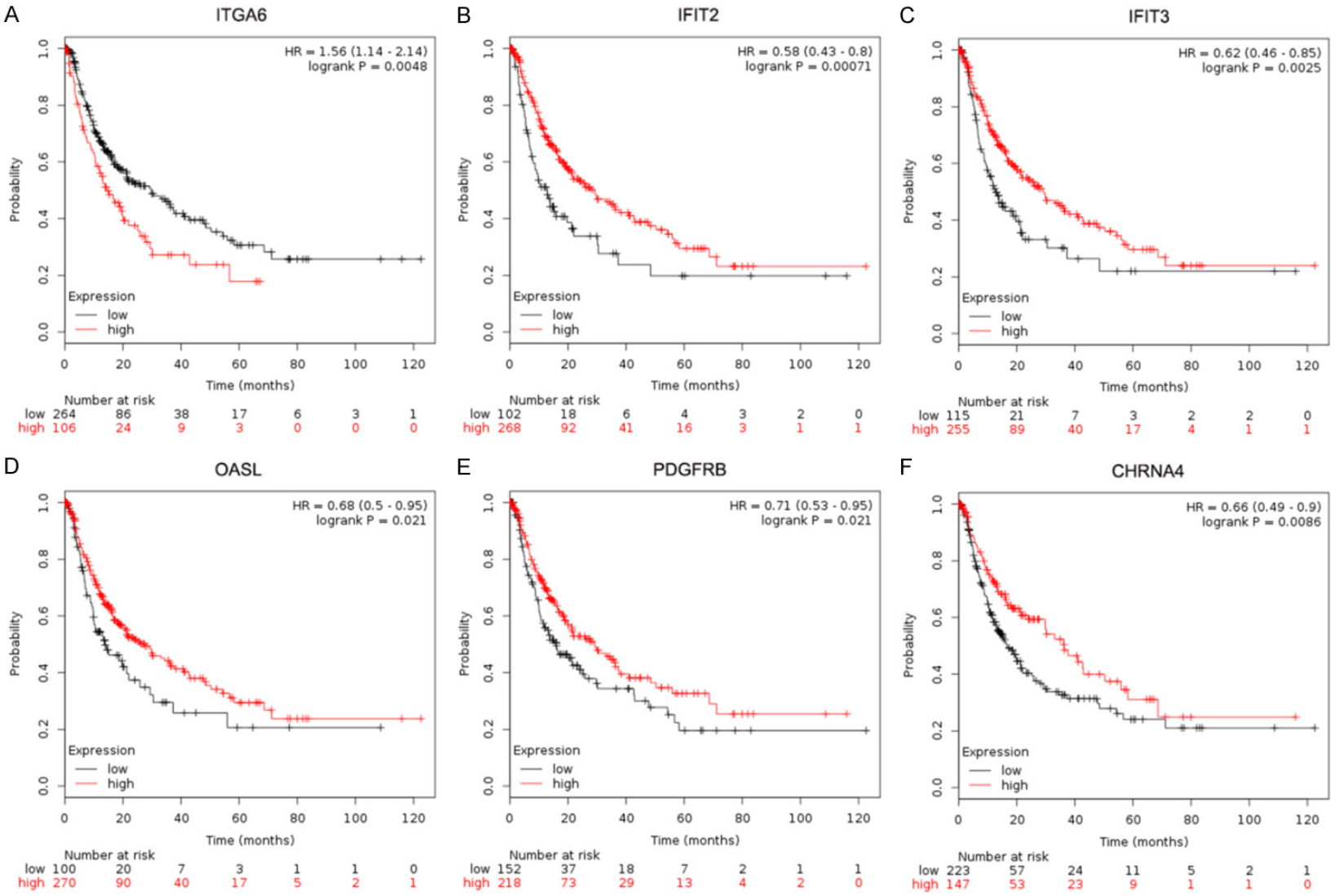

Figure 12. Kaplan-Meier survival curves for the prognostic significance of ten hub genes on progress free survival of liver cancer patients from the Cancer Genome Atlas. Liver cancer patients were split by the median expression value of hub genes. HR: hazard ratio. The survival outcome of patients in high expression group was marked in red line while the survival outcome of patients in low expression group was marked in black line.

attenuate the metastatic ability of HCC cells [33]. ITGB4 could cooperate with Slug to foster invasion and EMT of HCC cells [34]. Encouragingly, scatterplots for mRNA expression data in TCGA and GTEx suggested up-regulated expression levels of mRNA for ITGA6 and ITGB4; IHC pictures in the HPA database indicated up-regulated protein expression of ITGA6, which proved to some extent that ITGA6 and ITGB4 serve as oncogenes targeted by the five top NC-induced up-regulated miRNAs in HCC. With respect to the hub genes of the top five down-regulated miRNAs, the coordination of overexpressed lncRNA00364 and IFIT2 could damage proliferation of HCC cells [35]; IFIT3 was claimed to sensitize HCC patients to interferon-α (IFN-α) therapy [36]. Both IFIT2 and IFIT3 were revealed by Kaplan-Meier survival curves in the validation part of the present study to be prognostic factors portending a relatively favorable survival rate for HCC patients, strengthening the reliability of our results.

Limitations of this study should be acknowledged. First, we only detected the expression profile change of miRNA and mRNA upon treatment of NC in HCC xenografts originating from a single cell line, SMMC7721. For a better simulation of the biological background of HCC, more HCC cell lines should be collected for sequencing analysis. Second, regulating axes of NC-DEmiRNAs-DEmRNAs and TFs-DEmiRNAs-DEmRNAs established in this study were based on bioinformatics predictions and computations; as such, further in vitro or in vivo experiments should be carried out to verify the targeting relationships between NC, TF, DEmiRNAs, and DEmRNAs, as well as their functions in HCC. Previous studies have reported the cytotoxic effects of NC on healthy tissues and cell lines [37]. In the present work, we only focused on the anti-tumor function of NC in HCC. The side effects of NC in the treatment of HCC needed to be explored in future studies to judge and weigh the advantages and disadvantages of NC as potential therapeutic regime for HCC.

In conclusion, we discovered regulating axes of NC-DEmiRNAs-DEmRNAs and TFs-DEmiRNAs-DEmRNAs in HCC. NC might control expression of multiple miRNAs to influence the oncogenic or tumor suppressive functions of target genes such as ITGA6, ITGB4, IFIT2, and IFIT3, thereby playing the tumor-suppressive role in HCC.

Acknowledgements

This study was supported by Fund of National Natural Science Foundation of China (NSFC 81860717, NSFC81560489), Fund of Natural Science Foundation of Guangxi, China (2018GXNSFAA294025, 2017GXNSFAA198017), Guangxi Degree and Postgraduate Education Reform and Development Research Projects, China (JGY2019050), Guangxi Medical University Training Program for Distinguished Young Scholars, Scientific and Technological Innovation Training Program for College Students of the First Clinical Medical College of Guangxi Medical University and Medical Excellence Award Funded by the Creative Research Development Grant from the First Affiliated Hospital of Guangxi Medical University.

Disclosure of conflict of interest

None.

Address correspondence to: Gang Chen and Yi-Wu Dang, Department of Pathology, First Affiliated Hospital of Guangxi Medical University, 6 Shuangyong Road, Nanning 530021, Guangxi Zhuang Autonomous Region, China. Tel: +86-0771-5356534; Fax: +86-0771-5356534; E-mail: chengang@gxmu.edu.cn (GC); dangyiwu@126.com (YWD)

References

[1] Sheng Z, Wang X, Xu G, Shan G and Chen L. Analyses of a panel of transcripts identified from a small sample size and construction of RNA networks in hepatocellular carcinoma. Front Genet 2019; 10: 431.

[2] Forner A, Reig M and Bruix J. Hepatocellular carcinoma. Lancet 2018; 391: 1301-1314.

[3] Wang X, Liao X, Huang K, Zeng X, Liu Z, Zhou X, Yu T, Yang C, Yu L, Wang Q, Han C, Zhu G, Ye X and Peng T. Clustered microRNAs hsa-miR-221-3p/hsa-miR-222-3p and their targeted genes might be prognostic predictors for hepatocellular carcinoma. J Cancer 2019; 10: 2520-2533.

[4] Liu LM, Lin P, Yang H, Dang YW and Chen G. Gene profiling of HepG2 cells following nitidine chloride treatment: an investigation with microarray and connectivity mapping. Oncol Rep 2019; 41: 3244-3256.

[5] Shi Y, Cao T, Sun Y, Xia J, Wang P and Ma J. Nitidine hloride inhibits cell proliferation and invasion via downregulation of YAP expression in prostate cancer cells. Am J Transl Res 2019; 11: 709-720.

[6] Pan X, Han H, Wang L, Yang L, Li R, Li Z, Liu J, Zhao Q, Qian M, Liu M and Du B. Nitidine chloride inhibits breast cancer cells migration and invasion by suppressing c-Src/FAK associated signaling pathway. Cancer Lett 2011; 313: 181-191.
[7] Chen J, Wang J, Lin L, He L, Wu Y, Zhang L, Yi Z, Chen Y, Pang X and Liu M. Inhibition of STAT3 signaling pathway by nitidine chloride suppressed the angiogenesis and growth of human gastric cancer. Mol Cancer Ther 2012; 11: 277-287.
[8] Liao J, Xu T, Zheng JX, Lin JM, Cai QY, Yu DB and Peng J. Nitidine chloride inhibits hepatocellular carcinoma cell growth in vivo through the suppression of the JAK1/STAT3 signaling pathway. Int J Mol Med 2013; 32: 79-84.
[9] Ou X, Lu Y, Liao L, Li D, Liu L, Liu H and Xu H. Nitidine chloride induces apoptosis in human hepatocellular carcinoma cells through a pathway involving p53, p21, Bax and Bcl-2. Oncol Rep 2015; 33: 1264-1274.
[10] Wu P, Xiao Y, Guo T, Wang Y, Liao S, Chen L and Liu Z. Identifying miRNA-mRNA pairs and novel miRNAs from hepatocelluar carcinoma mirnomes and TCGA database. J Cancer 2019; 10: 2552-2559.
[11] Lv L, Wang X and Ma T. MicroRNA-944 inhibits the malignancy of hepatocellular carcinoma by directly targeting IGF-1R and deactivating the PI3K/Akt signaling pathway. Cancer Manag Res 2019; 11: 2531-2543.
[12] Liu LM, Xiong DD, Lin P, Yang H, Dang YW and Chen G. DNA topoisomerase 1 and 2A function as oncogenes in liver cancer and may be direct targets of nitidine chloride. Int J Oncol 2018; 53: 1897-1912.
[13] Assi SA, Bonifer C and Cockerill PN. Rewiring of the transcription factor network in acute myeloid leukemia. Cancer Inform 2019; 18: 1176935119859863.
[14] Jiang L, Yu X, Ma X, Liu H, Zhou S, Zhou X, Meng Q, Wang L and Jiang W. Identification of transcription factor-miRNA-lncRNA feed-forward loops in breast cancer subtypes. Comput Biol Chem 2019; 78: 1-7.
[15] Jiang W, Mitra R, Lin CC, Wang Q, Cheng F and Zhao Z. Systematic dissection of dysregulated transcription factor-miRNA feed-forward loops across tumor types. Brief Bioinform 2016; 17: 996-1008.
[16] Tong Z, Cui Q, Wang J and Zhou Y. TransmiR v2.0: an updated transcription factor-microRNA regulation database. Nucleic Acids Res 2019; 47: D253-D258.
[17] Pathan M, Keerthikumar S, Ang CS, Gangoda L, Quek CY, Williamson NA, Mouradov D, Sieber OM, Simpson RJ, Salim A, Bacic A, Hill AF, Stroud DA, Ryan MT, Agbinya JI, Mariadason JM, Burgess AW and Mathivanan S. FunRich: an open access standalone functional enrichment and interaction network analysis tool. Proteomics 2015; 15: 2597-2601.
[18] Liu N, Li P, Zang S, Liu Q, Ma D, Sun X and Ji C. Novel agent nitidine chloride induces erythroid differentiation and apoptosis in CML cells through c-Myc-miRNAs axis. PLoS One 2015; 10: e0116880.
[19] Jiang W, Wen D, Gong L, Wang Y, Liu Z and Yin F. Circular RNA hsa_circ_0000673 promotes hepatocellular carcinoma malignance by decreasing miR-767-3p targeting SET. Biochem Biophys Res Commun 2018; 500: 211-216.
[20] Zhu L, Liu Y, Chen Q, Yu G, Chen J, Chen K, Yang N, Zeng T, Yan S, Huang A and Tang H. Long-noncoding RNA colorectal neoplasia differentially expressed gene as a potential target to upregulate the expression of IRX5 by miR-136-5P to promote oncogenic properties in hepatocellular carcinoma. Cell Physiol Biochem 2018; 50: 2229-2248.
[21] Zhao S, Li J, Zhang G, Wang Q, Wu C, Zhang Q, Wang H, Sun P, Xiang R and Yang S. Exosomal miR-451a functions as a tumor suppressor in hepatocellular carcinoma by targeting LPIN1. Cell Physiol Biochem 2019; 53: 19-35.
[22] Kabacaoglu D, Ruess DA, Ai J and Algul H. NF-kappaB/Rel transcription factors in pancreatic cancer: focusing on RelA, c-Rel, and RelB. Cancers (Basel) 2019; 11: E937.
[23] Di W, Weinan X, Xin L, Zhiwei Y, Xinyue G, Jinxue T and Mingqi L. Long noncoding RNA SNHG14 facilitates colorectal cancer metastasis through targeting EZH2-regulated EPHA7. Cell Death Dis 2019; 10: 514.
[24] Gui B, Gui F, Takai T, Feng C, Bai X, Fazli L, Dong X, Liu S, Zhang X, Zhang W, Kibel AS and Jia L. Selective targeting of PARP-2 inhibits androgen receptor signaling and prostate cancer growth through disruption of FOXA1 function. Proc Natl Acad Sci U S A 2019; 116: 14573-14582.
[25] Tu CC, Kumar VB, Day CH, Kuo WW, Yeh SP, Chen RJ, Liao CR, Chen HY, Tsai FJ, Wu WJ and Huang CY. Estrogen receptor alpha (ESR1) over-expression mediated apoptosis in Hep3B cells by binding with SP1 proteins. J Mol Endocrinol 2013; 51: 203-212.
[26] Li Y, Fu Y, Hu X, Sun L, Tang D, Li N, Peng F and Fan XG. The HBx-CTTN interaction promotes cell proliferation and migration of hepatocellular carcinoma via CREB1. Cell Death Dis 2019; 10: 405.
[27] Luo W, Zhu X, Liu W, Ren Y, Bei C, Qin L, Miao X, Tang F, Tang G and Tan S. MYC associated zinc finger protein promotes the invasion and metastasis of hepatocellular carcinoma by inducing epithelial mesenchymal transition. Oncotarget 2016; 7: 86420-86432.

[28] Fang T, Cui M, Sun J, Ge C, Zhao F, Zhang L, Tian H, Zhang L, Chen T, Jiang G, Xie H, Cui Y, Yao M, Li H and Li J. Orosomucoid 2 inhibits tumor metastasis and is upregulated by CCAAT/enhancer binding protein beta in hepatocellular carcinomas. Oncotarget 2015; 6: 16106-16119.

[29] Shigekawa Y, Hayami S, Ueno M, Miyamoto A, Suzaki N, Kawai M, Hirono S, Okada KI, Hamamoto R and Yamaue H. Overexpression of KDM5B/JARID1B is associated with poor prognosis in hepatocellular carcinoma. Oncotarget 2018; 9: 34320-34335.

[30] Hishida M, Nomoto S, Inokawa Y, Hayashi M, Kanda M, Okamura Y, Nishikawa Y, Tanaka C, Kobayashi D, Yamada S, Nakayama G, Fujii T, Sugimoto H, Koike M, Fujiwara M, Takeda S and Kodera Y. Estrogen receptor 1 gene as a tumor suppressor gene in hepatocellular carcinoma detected by triple-combination array analysis. Int J Oncol 2013; 43: 88-94.

[31] Sun M, Zhang N, Wang X, Li Y, Qi W, Zhang H, Li Z and Yang Q. Hedgehog pathway is involved in nitidine chloride induced inhibition of epithelial-mesenchymal transition and cancer stem cells-like properties in breast cancer cells. Cell Biosci 2016; 6: 44.

[32] Cheng Z, Guo Y, Yang Y, Kan J, Dai S, Helian M, Li B, Xu J and Liu C. Nitidine chloride suppresses epithelial-to-mesenchymal transition in osteosarcoma cell migration and invasion through Akt/GSK-3beta/Snail signaling pathway. Oncol Rep 2016; 36: 1023-1029.

[33] Lv G, Lv T, Qiao S, Li W, Gao W, Zhao X and Wang J. RNA interference targeting human integrin alpha6 suppresses the metastasis potential of hepatocellular carcinoma cells. Eur J Med Res 2013; 18: 52.

[34] Li XL, Liu L, Li DD, He YP, Guo LH, Sun LP, Liu LN, Xu HX and Zhang XP. Integrin beta4 promotes cell invasion and epithelial-mesenchymal transition through the modulation of Slug expression in hepatocellular carcinoma. Sci Rep 2017; 7: 40464.

[35] Tang WG, Hu B, Sun HX, Sun QM, Sun C, Fu PY, Yang ZF, Zhang X, Zhou CH, Fan J, Ren N and Xu Y. Long non-coding RNA00364 represses hepatocellular carcinoma cell proliferation via modulating p-STAT3-IFIT2 signaling axis. Oncotarget 2017; 8: 102006-102019.

[36] Yang Y, Zhou Y, Hou J, Bai C, Li Z, Fan J, Ng IOL, Zhou W, Sun H, Dong Q, Lee JMF, Lo CM, Man K, Yang Y, Li N, Ding G, Yu Y and Cao X. Hepatic IFIT3 predicts interferon-alpha therapeutic response in patients of hepatocellular carcinoma. Hepatology 2017; 66: 152-166.

[37] Li W, Yin H, Bardelang D, Xiao J, Zheng Y and Wang R. Supramolecular formulation of nitidine chloride can alleviate its hepatotoxicity and improve its anticancer activity. Food Chem Toxicol 2017; 109: 923-929.

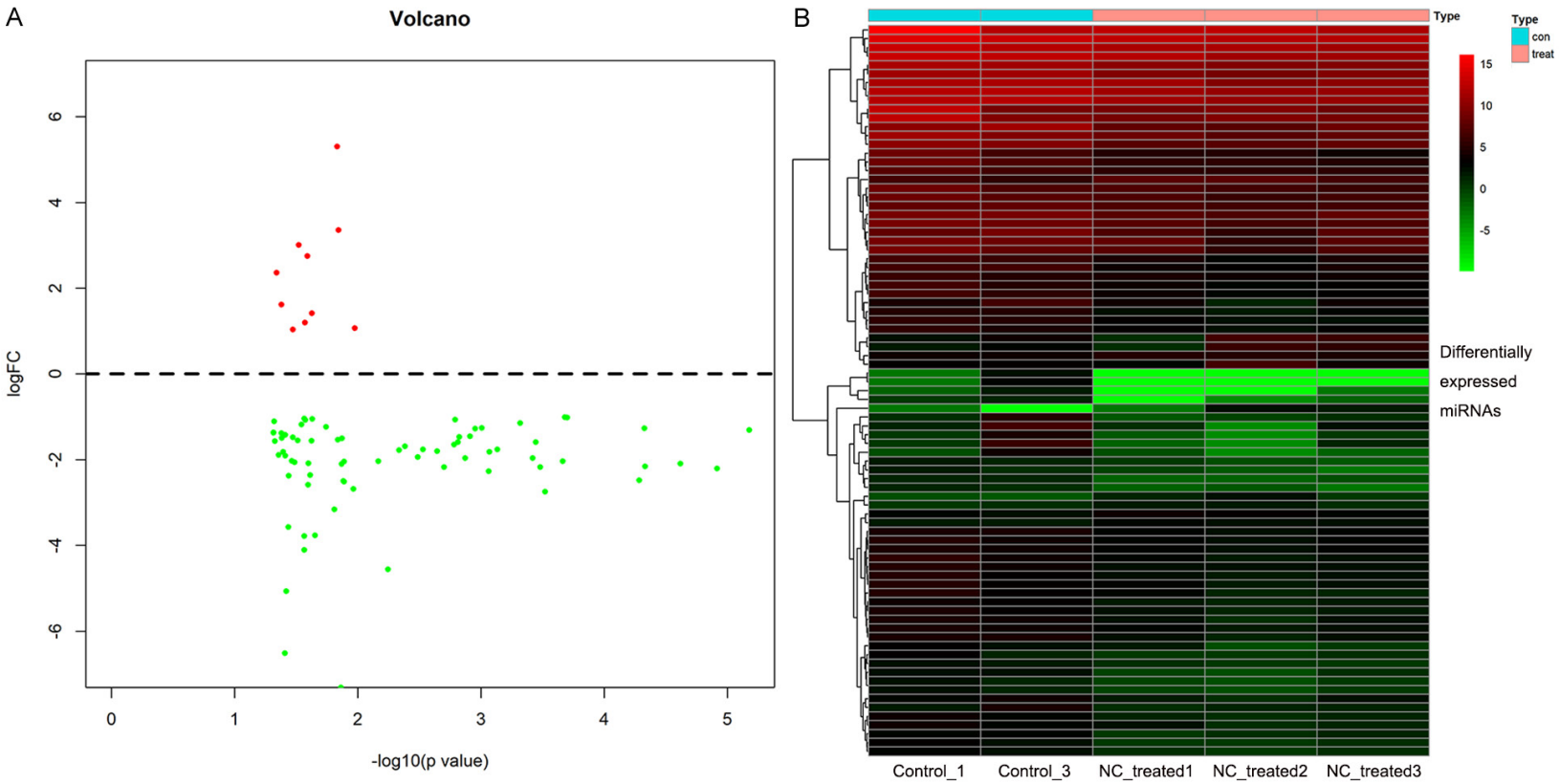

Supplementary Figure 1. Differentially expressed miRNAs (DEmiRNAs) in nitidine chloride (NC)-treated samples. A. Volcano plot. Up-regulated and down-regulated DEmiRNAs are represented as red and green dots, respectively. B. Heatmap. The color spectrum ranging from green to red reflect the expression of 83 DEmiRNAs from low to high.

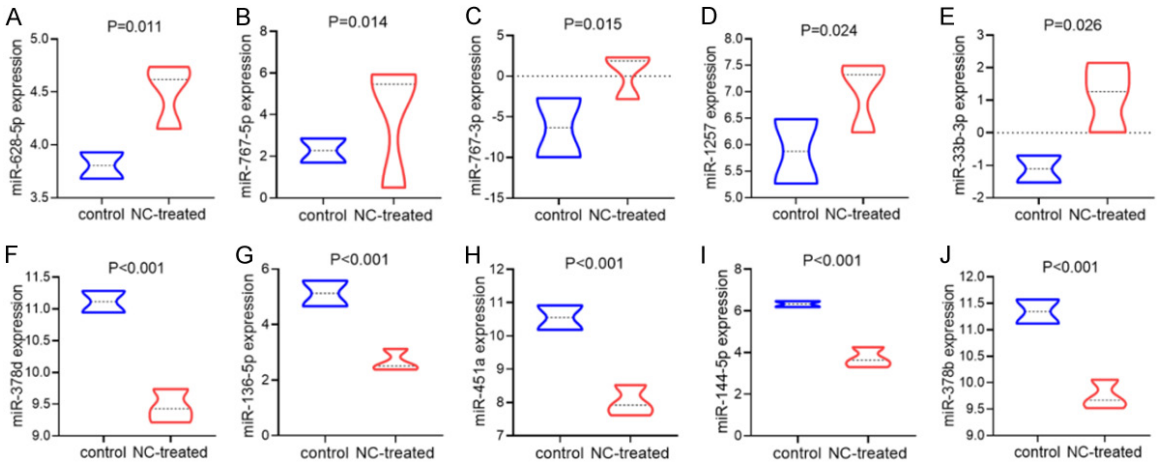

Supplementary Figure 2. Violin plots of expression patterns of the ten most significant differentially expressed miRNAs (DEmiRNA) in control and nitidine chloride (NC)-treated samples. A: Differential expression of miR-628-5p in three NC-treated and two control groups; B: Differential expression of miR-767-5p in three NC-treated and two control groups; C: Differential expression of miR-767-3p in three NC-treated and two control groups; D: Differential expression of miR-1257 in three NC-treated and two control groups; E: Differential expression of miR-33b-3p in three NC-treated and two control groups; F: Differential expression of miR-378d in three NC-treated and two control groups; G: Differential expression of miR-136-5p in three NC-treated and two control groups; H: Differential expression of miR-451a in three NC-treated and two control groups; I: Differential expression of miR-144-5p in three NC-treated and two control groups; J: Differential expression of miR-378b in three NC-treated and two control groups.

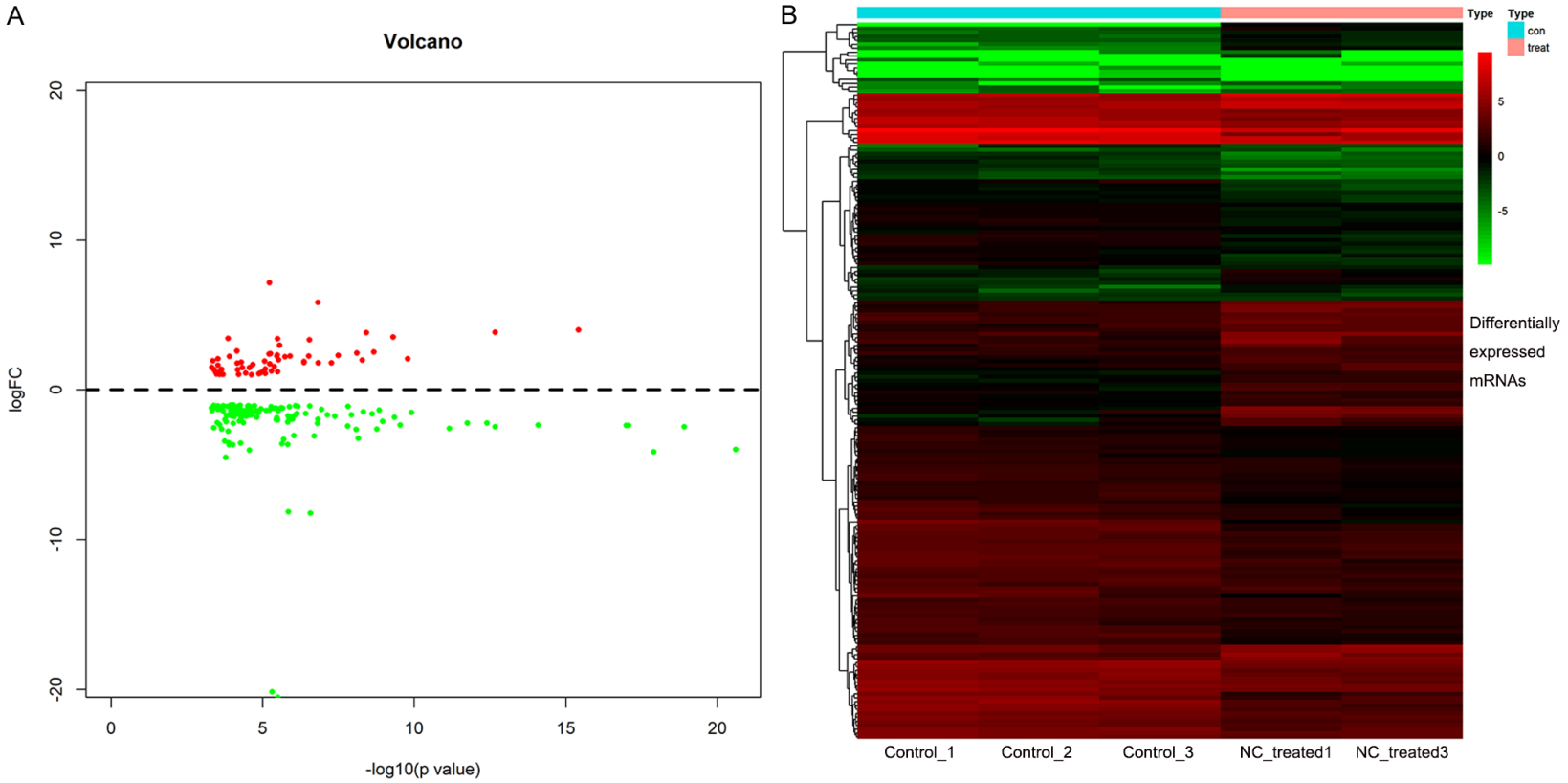

Supplementary Figure 3. Differentially expressed mRNAs (DEmRNAs) in nitidine chloride (NC)-treated samples. A. Volcano plot. Up-regulated and down-regulated DEmRNAs are represented as red and green dots, respectively. B. Heatmap. The color spectrum ranging from green to red reflect the expression of DEmRNAs from low to high. DEmRNAs were represented as different bars. Samples in control and NC-treated groups were distinguished by blue and red.

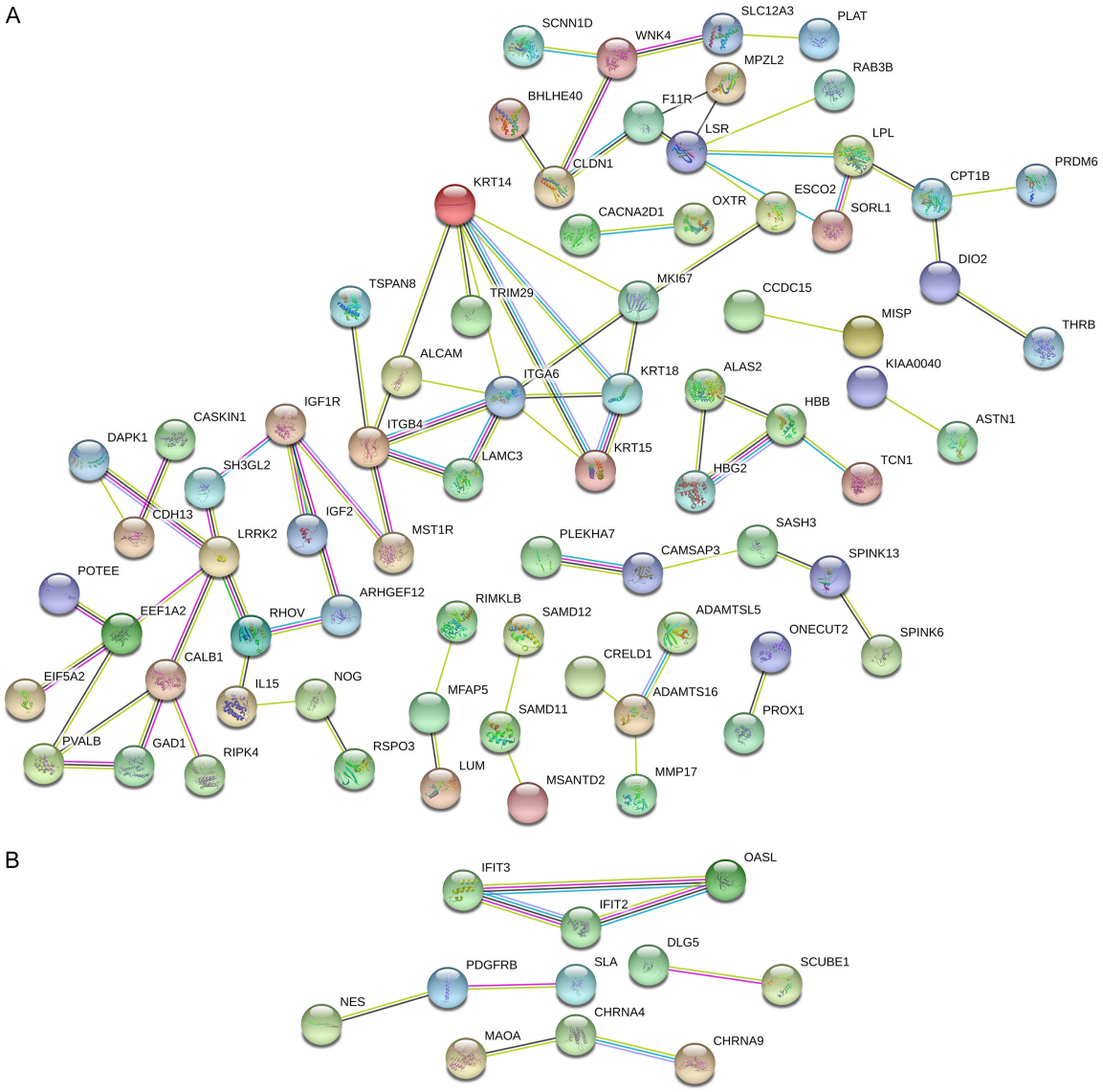

Supplementary Figure 4. Protein-to-protein interaction (PPI) networks for potential target genes of the five top up-regulated miRNAs and the five top down-regulated miRNAs. A: The color of the nodes represents the shell of interactors, and the number of edges between two nodes reflects the number of sources of interaction between potential target genes of the five top up-regulated miRNAs. B: The color of nodes represents the shell of interactors, and the number of edges between two nodes reflects the number of sources of interaction between potential target genes of the five top down-regulated miRNAs.

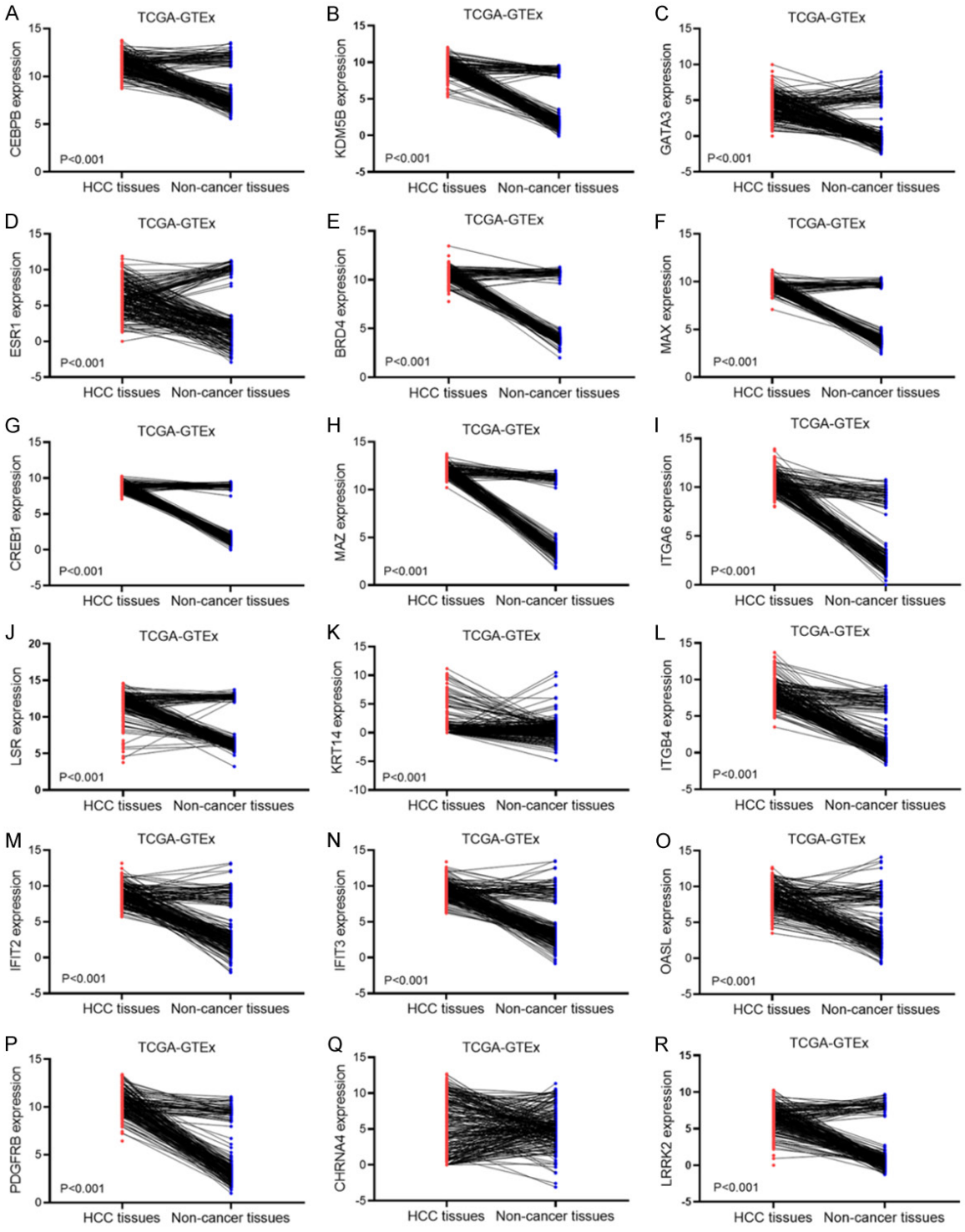

Supplementary Figure 5. RNA expression difference of hub genes and TFs in hepatocellular carcinoma (HCC) and normal tissues from GEPIA. A-R correspond to RNA expression of CEBPB, KDM5B, GATA3, ESR1, BRD4, MAX, CREB1, MAZ, ITGA6, LSR, KRT14, ITGB4, IFIT2, IFIT3, OASL, PDGFRB, CHRNA4 and LRRK2 in 369 HCC and 160 normal tissues. HCC tissues were marked in red while non-cancer tissues were marked in blue.